# Chemically exfoliated single-layer $MoS_2$: Stability, lattice dynamics, and catalytic adsorption from first principles

Matteo Calandra*
*Université Pierre et Marie Curie, IMPMC, CNRS UMR7590, 4 place Jussieu, 75005 Paris, France*
(Received 12 November 2013; published 18 December 2013)

Chemically and mechanically exfoliated $MoS_2$ single-layer samples have substantially different properties. While mechanically exfoliated single-layers are monophase(1H polytype with Mo in trigonal prismatic coordination), the chemically exfoliated samples show coexistence of three different phases, 1H, 1T (Mo in octahedral coordination), and 1T′ (a distorted $2 \times 1$ 1T superstructure). By using first-principles calculations, we investigate the energetics and the dynamical stability of the three phases. We show that the 1H phase is the most stable one, while the metallic 1T phase, strongly unstable, undergoes a phase transition towards a metastable and insulating 1T′ structure composed of separated zigzag chains. We calculate electronic structure, phonon dispersion, Raman frequencies, and intensities for the 1T′ structure. We provide a microscopical description of the $J_1$, $J_2$, and $J_3$ Raman features that were first detected more than 20 years ago but have remained unexplained up to now. Finally, we show that H adsorbates, which are naturally present at the end of the chemical exfoliation process, stabilize the 1T′ over the 1H one.

DOI: 10.1103/PhysRevB.88.245428 PACS number(s): 62.23.Kn, 63.22.−m, 68.43.Bc

## I. INTRODUCTION

Bulk transition-metal dichalcogenides (TMD) are layered van der Waals solids displaying remarkable properties that are promising both for fundamental research and for technological applications. Metallic bulk TMD, such as $NbSe_2$, present the coexistence of the charge-density wave and superconductivity,[1,2] while insulating TMD ($MoS_2$, $WS_2$) are flexible, have high mobilities, and are routinely used in flexible electronics.

Since the pioneering work of Frindt and coworkers[3–6] and the successive developments in the fields of mechanical[7] and liquid[8] exfoliation, it has been possible to obtain free-standing or supported single-layer TMD. These monolayers are the inorganic analog of graphene and display a rich chemistry[9] that makes them attractive for energy-storage applications. Insulating single-layer TMD have much lower mobilities[10,11] than graphene but are nevertheless interesting for nanoelectronics, mainly due to the presence of a finite band gap.

In this context, $MoS_2$ is considered one of the most promising materials.[12] The most stable polytype of bulk $MoS_2$ is 2H (molybdenite), where each Mo has a trigonal prismatic coordination with the nearby S atoms. Mechanical exfoliation of bulk 2H $MoS_2$ leads to the formation of single-layer samples with the same local coordination (here labeled 1H $MoS_2$). In chemically exfoliated samples the situation is different. In the first step of chemical exfoliation of bulk 2H $MoS_2$, Li atoms are intercalated between the layers. The Li intercalation stabilize a 1T $Li_xMoS_2$ polytype where each Mo is octahedrally coordinated with the nearby S atoms. Subsequent hydration with excess water and ultrasonication lead to the separation of the layers via LiOH formation and synthesis of large-area single-layer $MoS_2$ samples.[4]

The properties of chemically exfoliated $MoS_2$ single layers are poorly understood. Recently, it has been shown that these samples are actually composed of heterostructures of 1H, 1T, and 1T-distorted (labeled 1T′) $MoS_2$ phases.[13] The 1T′ phase is a $2 \times 1$ superstructure of the 1T phase formed by zigzag chains. Remarkably, the three phases coexist in the same sample and have substantially different conducting properties as the 1T phase is metallic while 1H and 1T′ are insulating.[14] Upon mild annealing at 200–300 °C the 1T and 1T′ phases disappear and transform into the 1H one. Exposure to a 60–80-keV electron beam induces S vacancies[15] and transforms the 1T′ phase into the 1T one.[13,16] Finally, it is important to remark that chemically exfoliated single layers are covered with adsorbates that can play some role in stabilizing one structure or the other.

The dynamical properties of the 1T′ phase are not understood. For example, while it is well established that the high-energy optical Raman spectra of the 1H phase are composed of two prominent peaks, attributed to the $E_{2g}$ mode at $\approx$385 $cm^{-1}$ and to the $A_{1g}$ mode at $\approx$403 $cm^{-1}$,[17] little is known about the Raman spectra of the 1T′ phase. Raman measurements[18] on freshly prepared single-layers with dominant 1T′ phase show that the $E_{2g}$ peak is missing, while at least five additional peaks appear at lower energies (some of these peaks are labeled $J_1$, $J_2$, $J_3$). Nothing is known on the phonon displacements generating these features.

In this work we study the stability, the electronic structure, and the dynamical properties of the 1T and 1T′ phases in single-layer $MoS_2$ by using density functional theory (DFT) calculations. We show that the metallic 1T phase is dynamically unstable. We find distorted structures with $2 \times 1$ (1T′$MoS_2$) and $2 \times 2$ (labeled 1T″$MoS_2$) real-space periodicities that have lower energies than the 1T one. Both 1T′ and 1T″ structures are, however, substantially higher in energy than the 1H $MoS_2$ phase (see Fig. 1 for a plot of the crystal structure of the different phases).

We then fully characterize the distorted 1T′ phase found in experiments on chemically exfoliated $MoS_2$ by obtaining its electronic structure, phonon dispersion, and Raman intensities. Finally, we study catalytic absorption in the 1T′ phase and show that H adsorbates stabilize the 1T′ phase with respect to all the others.

This paper is organized as follows. In Sec. II we describe the technical details of the calculation. In Sec. III A we analyze the stability of octahedral phases with respect to the trigonal

 

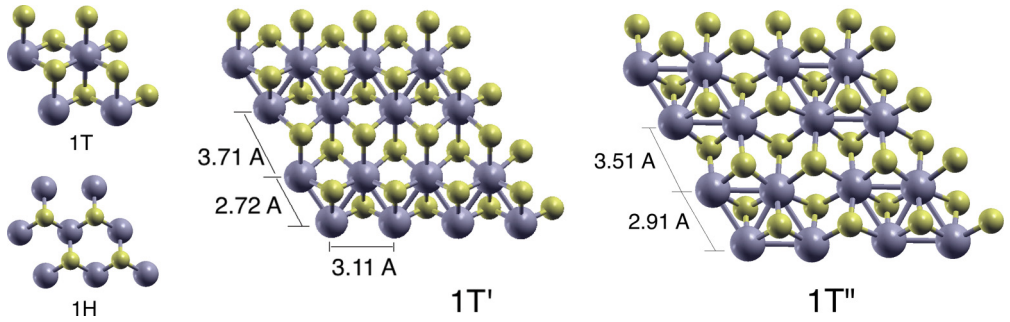


FIG. 1. (Color online) Phases of chemically exfoliated $MoS_2$. The 1H phase has trigonal prismatic coordination and is the most stable among all polytypes. The 1T, 1T′, and 1T″ polytypes all have octahedral coordination. The 1T′ polytype is the lowest-energy polytype among those with octahedral coordination. The in-plane Mo-Mo distance is 3.193 and 3.183 Å for the 1T′ and 1H structures, respectively.

prismatic ones, and in Sec. III B we study the Raman spectrum of the distorted 1T′ phase. Finally, in Sec. III C we study catalytic adsorption of hydrogen and its effect on the structural and electronic properties of the different structures.

## II. TECHNICAL DETAILS

The results reported in the present paper were obtained from first-principles density functional theory in the generalized gradient approximation.[19] The QUANTUM ESPRESSO[20] package was used with norm-conserving pseudopotentials and a plane-wave cutoff energy of 90 Ry. Semicore states were included in the Mo pseudopotential. The electronic structure calculations were performed by using $24 \times 24$, $12 \times 24$, and $12 \times 12$ electron-momentum grids for the 1T, 1T′, and 1T″ phases, respectively. For the metallic 1T structure we use a Hermitian-Gaussian smearing of 0.01 Ry. The phonon dispersion of the 1T phase was calculated by Fourier interpolating dynamical matrices calculated on a $8 \times 8$ phonon-momentum grid and on a $24 \times 24$ electron-momentum grid. The Raman intensity calculation for the 1T′ phase was performed on an $8 \times 16$ electron-momentum grid. The phonon dispersion calculation for the 1T′ structure was performed using a $4 \times 4$ phonon momentum grid.

## III. RESULTS

### A. Stability of octahedral phases

We first investigate the relative stability of 2H and 1T phases in Fig. 1. As expected, we find that the 1H $MoS_2$ phase is the most stable one, with a lower energy of 0.83 eV/Mo atom with respect to the 1T one. The electronic structure calculation of the 1T structure in Fig. 2 shows that this polytype is indeed metallic. Different from the 1H case, here the spin-orbit coupling is very weak, and from now on it will be neglected.

As the energy difference between the 1T and 2H phases is more than 30 times larger than the 200–300 K annealing temperature necessary to transform the 1T phase into the 2H one, the experimental detection of the 1T and 1T′ phases cannot be inferred from the total energy difference between the two. It has been suggested that the 1T phase is metastable and, as a consequence, an energetic barrier occurs between

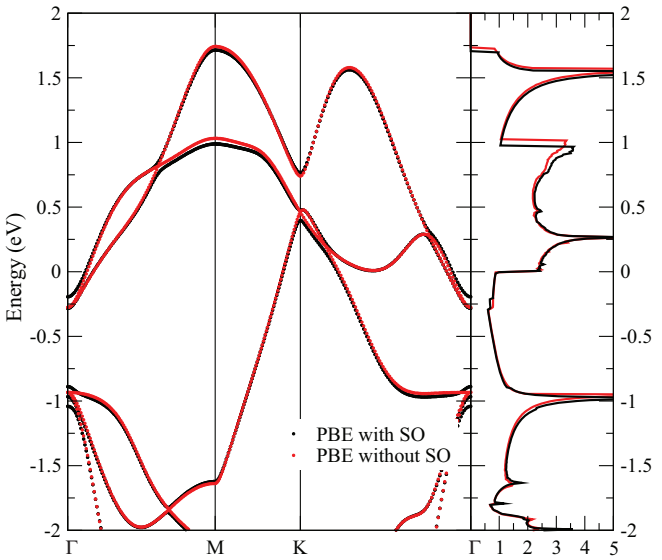


FIG. 2. (Color online) Electronic structure and density of states (states/eV/cell) of the 1T $MoS_2$ phase with and without spin-orbit coupling. The energy is plotted with respect to the Fermi level.

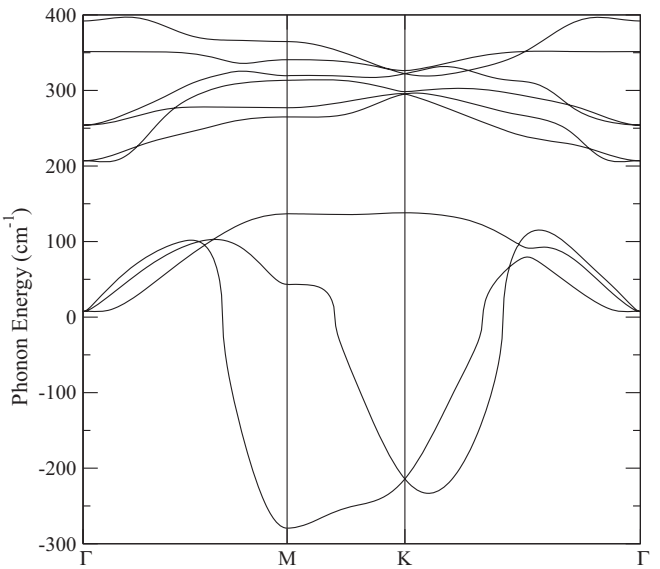


FIG. 3. Phonon dispersion of the 1T $MoS_2$ phase showing a dynamical instability at the zone border.

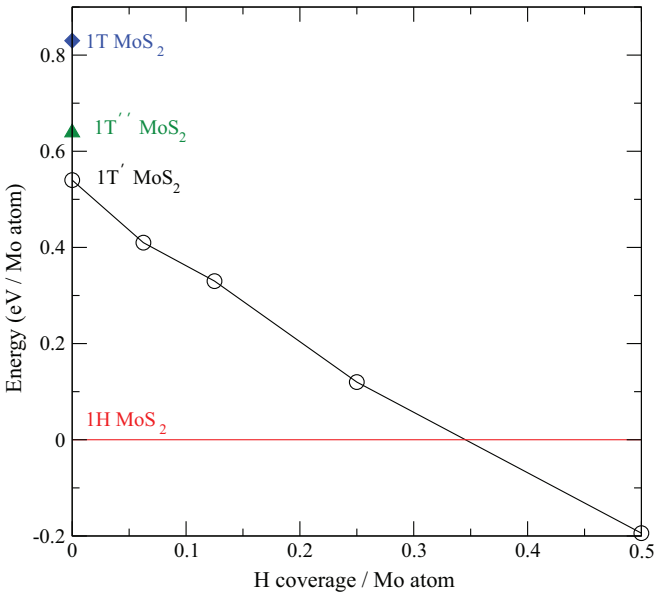


FIG. 4. (Color online) Stability of different $MoS_2$ structures with respect to the 1H polytype and as a function of H coverage per Mo atom.

the two.[9] To verify this hypothesis, we calculate the phonon dispersion for the 1T phase. We find that the 1T structure is dynamically unstable (see Fig. 3) at the zone border, with the largest instability at the $M$ point of the hexagonal lattice. This distortion is compatible with a $2 \times 1$ superstructure. To identify the lowest-energy superstructure, we perform calculations on a $2 \times 1$ supercell by displacing the atoms along the direction given by the phonon displacement of the most unstable mode at $M$. We find that substantial energy (0.19 eV/Mo) is gained by the distortion. We then start from this distorted structure and perform full structural optimization of internal coordinates and of the two-dimensional (2D) cell. As shown in Fig. 4, we find the stabilization of an octahedrally coordinated structure composed of zigzag chains, with an energy gain of 0.29 eV/Mo with respect to the 1T phase. Structural parameters of the zigzag distorted structure are given in Table I. Here we remark that the shortest distance between Mo atoms belonging to the same chain is ≈2.72 Å, while the shortest distance between atoms on different chains is ≈3.71 Å. The angle between the Mo atoms in the chain is ≈69.64°. The in-plane nearest-neighbor Mo-Mo distance of the 1T′ structure is almost identical to the nearest-neighbor distance of Mo atoms in bcc Mo,[21] which is 2.728 Å. On the contrary in the 1T structure the Mo-Mo bond is 3.193 Å, substantially elongated with respect to the Mo-Mo nearest-neighbor distance in bcc Mo.

TABLE I. Atomic coordinates with respect to the direct axis for the 1T′ structure. The lengths of the two direct lattice vectors of the two-dimensional lattice are identified by $a = 6.411$ Å, $b = 3.111$ Å. The angle between them $\gamma = 119.034°$.

| Atom | $x$ | $y$ | $z$ |
|---|---|---|---|
| Mo | 0.0508948 | 0.0508948 | 0.0051972 |
| S | 0.1662841 | 0.6662835 | 0.1240922 |
| S | 0.3337158 | 0.3337161 | −0.1240922 |
| Mo | 0.4491051 | −0.0508948 | −0.0051972 |
| S | 0.6714116 | 0.6714108 | 0.0957802 |
| S | 0.8285883 | 0.3285888 | −0.0957802 |

The devised 1T′ structure closely resembles that detected in experiments on chemically exfoliated samples.[13]

The electronic density of states of the distorted structure is shown in Fig. 5. The distortion opens a very small gap (≈0.045 eV) that makes the system insulating. The formation of zigzag chains is actually very similar to the standard Peierls dimerization in one-dimensional systems; that is, the system gains energy in opening a gap. The Peierls distortion reduces the dimensionality of the 2D layer that is now broken into one-dimensional (1D) zigzag chains. This is at odds with most bulk metallic transition-metal dichalcogenides where the charge-density-wave state coexists with metallicity and superconductivity.[1] However, given the large energy gain and the strong bond deformation involved in this distortion, the transition to 1D zigzag chains has to be considered more a real structural transition than a charge-density wave.

As the energy difference between the 1T′ and the 1H structures is large (0.54 eV/Mo), we perform additional structural optimization on the $2 \times 2$ supercell to see if other superstructures can be stabilized. We do indeed find another distorted structure formed by a Mo rhombus (1T″ $MoS_2$; see Fig. 1 and Table II) that is 0.19 eV lower in energy than the 1T structure but is still higher than both the 1T′ and 1H ones. Interestingly, in past experimental works on chemically exfoliated $MoS_2$ samples,[6] a similar 1T″ structure was proposed as the most stable one in the monolayer.

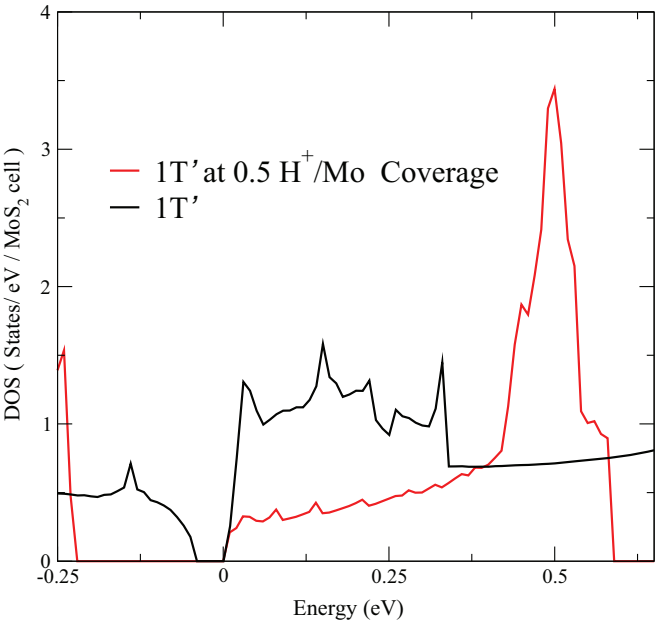


FIG. 5. (Color online) Electronic density of states of the 1T′ structure at 0 and 0.5 H/Mo coverage. The zero of the energy has been set to the bottom of the conduction band.

TABLE II. Coordinates of the 12 atoms in the 1T″ unit cell with respect to the direct lattice vectors. The lengths of the two direct lattice vectors of the two-dimensional lattice are identified by $a = b = 6.422$ Å. The angle between the two is $\gamma = 119.331^\circ$.

| Atom | $x$ | $y$ | $z$ |
|---|---|---|---|
| Mo | 0.022531337 | 0.022531337 | 0.0 |
| S | 0.317728127 | 0.651403657 | 0.056424736 |
| S | 0.651403657 | 0.317728127 | −0.056424736 |
| Mo | 0.465000117 | 0.001783220 | −0.000455305 |
| S | 0.815301793 | 0.651805630 | 0.049761398 |
| S | 1.150643861 | 0.316295157 | −0.062393003 |
| Mo | 0.444399776 | 0.444399776 | 0.0 |
| S | 0.814643878 | 1.148463448 | 0.056499460 |
| S | 1.148463448 | 0.814643878 | −0.056499460 |
| Mo | 0.001783220 | 0.465000117 | 0.000455305 |
| S | 0.316295157 | 1.150643861 | 0.062393003 |
| S | 0.651805630 | 0.815301793 | −0.049761398 |

### B. Raman spectra of the distorted 1T′ phase

In order to substantiate that the 1T′ structure determined theoretically is the same as the experimental one, we calculate the phonon frequencies at the zone center and the first-order Raman intensities for the 1T′ structure. We also give a complete interpretation of Raman spectra in chemically exfoliated samples that is currently lacking in the literature.

In 1H $MoS_2$, at high energy, only two Raman peaks are seen, namely, the $E_{2g}$ mode at ≈385 $cm^{-1}$ and the $A_{1g}$ mode at ≈403 $cm^{-1}$ (see Ref. 17). The experimental Raman spectra of the 1T′ phase show two main variations with respect to H polytypes: (i) the $E_{2g}$ peak disappears, and (ii) five additional peaks occur (see Table III). Due to the reduced symmetry of the 1T′ structure, we do indeed find several Raman active peaks and a very rich spectrum. The $E_{2g}$ peak is missing, and the additional calculated Raman peaks can be associated with the experimental ones with a high degree of accuracy.

In our calculation the peak with the largest intensity is the so-called $J_2$ peak at 216 $cm^{-1}$(226 $cm^{-1}$ in experiment). This mode tends to shorten the distance between the two zigzag chains and to recover the 1H structure (see Fig. 6). In experiments[18] this mode has a much larger linewidth than all the others. This partly explains why the experimental height of the peak is substantially reduced with respect to the Raman intensity.

The so-called $J_1$ peak at 156 $cm^{-1}$ in experiments is actually composed of two different phonon modes 4 $cm^{-1}$ apart. The one at 147 $cm^{-1}$ is an antiphase out-of-plane shift of each stripe of Mo atoms inside the zig-zag chain. The mode at 151 $cm^{-1}$ is an in-plane shearing mode of one stripe of an atom with respect to the other inside a chain. The peaks at 233 $cm^{-1}$ and at 286 $cm^{-1}$ involve shifts of the S-atom layers with respect to the Mo atoms. The $J_3$ mode at 333 $cm^{-1}$, in excellent agreement with experiments, tends to break each zigzag chain in two stripes with a slight out-of-plane component. The mode at 350 $cm^{-1}$ compares favorably with the 358 $cm^{-1}$ peak detected in experiments, although in theory it has a too small intensity. Finally, the mode at 412 $cm^{-1}$ is nothing more than the usual $A_{1g}$ mode seen in the 1H polytype. The agreement between the calculated zone-center energies and the position of Raman peaks suggests that the devised structure closely resembles the experimental one. Some disagreement still exists between the calculated relative intensities and the experimental ones. However, it should be noted that Raman spectra on different samples[14,18] show substantially different Raman intensities, probably due either to the inhomogeneity of the samples that are composed of several phases or to the presence of adsorbates and vacancies.

Finally, in Fig. 7 we show the calculated phonon dispersion of the 1T′ structure that is dynamically stable, suggesting that an energy barrier does indeed exist between the 1H and 1T′ phases and that the 1T′ phase is metastable.

TABLE III. Calculated phonon frequencies (in $cm^{-1}$) and first-order Raman intensities of the 1T′ phase compared with experiments for both 1T′ and 1H phases. The intensities are normalized to the most intense peak. The incoming and outgoing light in the Raman experiment are assumed to be unpolarized. See Ref. 22 for more details on the definition of the Raman intensities.

| Theory ($cm^{-1}$) | Theory, intensity | Experiment[18] ($cm^{-1}$) | 1H $MoS_2$[17] ($cm^{-1}$) |
|---|---|---|---|
| 147 | 0.003 | | |
| 151 | 0.008 | 156 ($J_1$) | |
| 216 | 1.0 | 226 ($J_2$) | |
| 223 | 0.006 | | |
| 286 | 0.011 | 287 | |
| 333 | 0.033 | 333 ($J_3$) | |
| 350 | <0.001 | 358 | 385 ($E_{2g}$) |
| 412 | 0.13 | 408 | 403 ($A_{1g}$) |

### C. Catalytic adsorption

In order to justify the stabilization of the 1T′ crystal structure with respect to the 1H one detected in experiments, we study adsorption on the 1H, 1T, 1T′, and 1T″ phases. Single-layers $MoS_2$ samples at the end of the chemical exfoliation process are fully covered with adsorbates due to the hydration of $Li_xMoS_2$ with water. We focus on the simple case of H adsorption. We consider $4 \times 4$ supercells of the 1T and 2H phases, as well as $2 \times 4$ supercells of the 1T′ unit cell. We start by considering only one H ion at random positions on top of the $MoS_2$ layer and then perform several structural optimizations. We find that the H ion always binds to an S atom, similar to what happens in $WS_2$.[9] Indeed, in the absence of adsorbates, a positive (negative) charge resides on the Mo (S) atom,[23] as can also be inferred from the relative electronegativity of S and Mo. We then add a second H atom and find that two H atoms prefer to bind to different S atoms. Thus, we start the structural minimization runs by considering all the possible ways to bind H to different S atoms that are compatible with the supercell size.

By performing structural minimization, we find that at all H coverages the 1H structure retains its trigonal prismatic coordination. Similarly, even when higher in energy, the H-covered 1T′ structure never decays into the 1H one but preserves its zigzag structure, although the separation between the chains and the bonding inside the chain are affected

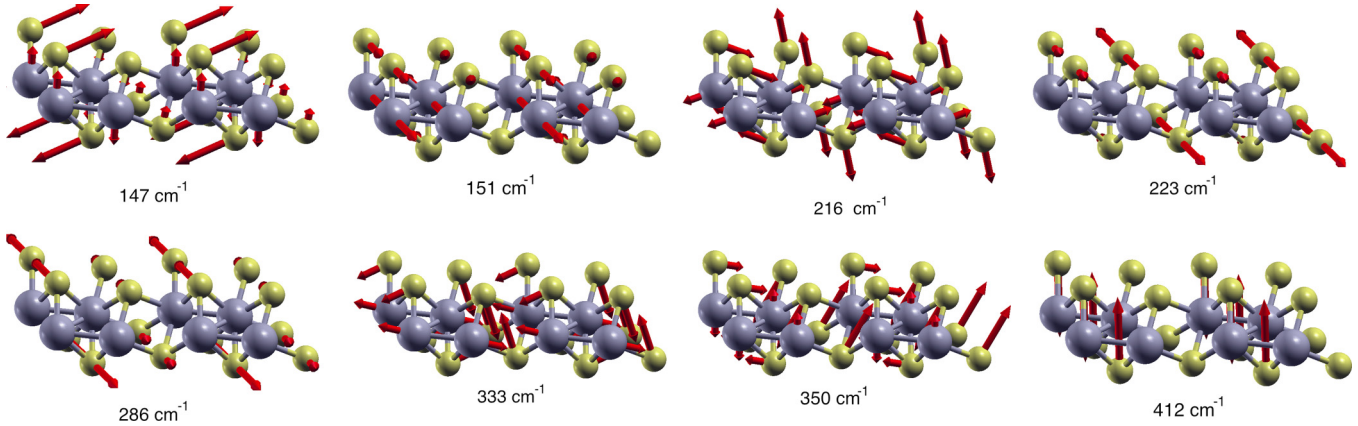


FIG. 6. (Color online) Raman active modes of the 1T′ $MoS_2$ single layer. The length of the arrows is proportional to the modulus of the phonon eigenvector.

by the H concentration. This confirms once more that an energy barrier does indeed occur between the 1H and 1T′ structures. Finally, we find that the H-covered 1T structure always decays into the H-covered 1T′ one, confirming the dynamical instability of the 1T phase towards 1T′. At large enough coverage, this is also what happens to the 1T″ structure, which also decays on 1T′.

In Fig. 4 we show the lowest-energy configuration of all phases with respect to the most stable configuration of the 1H structure at a given H coverage. We find that at H coverages superior to 0.35/Mo, the 1T′ phase is more stable than the 1H one. This suggests that in chemically exfoliated $MoS_2$ monolayers, the samples are divided into H-rich regions, where the 1T′ structure is stabilized, and H-poor regions, where the 1H phase is stabilized.

By comparing in detail the 1T′ structures at 0 and 0.5 H/Mo coverage (see Fig. 8), it is seen that upon H adsorption the separation between the chains strongly increases, as the shortest distance between Mo atoms on different chains is 3.91 Å(3.71 Å) at a coverage of 0 H/Mo (0.5 H/Mo). Furthermore, at a coverage of 0.5 H/Mo the Mo atoms do not lie on the same plane, as in the undistorted case, but are displaced above or below by ≈0.07 Å. The increased distance between the chains implies a larger band gap and more insulating character, as shown in Fig. 5. This agrees with experiments that found the zigzag chain structure is indeed insulating.[13,14]

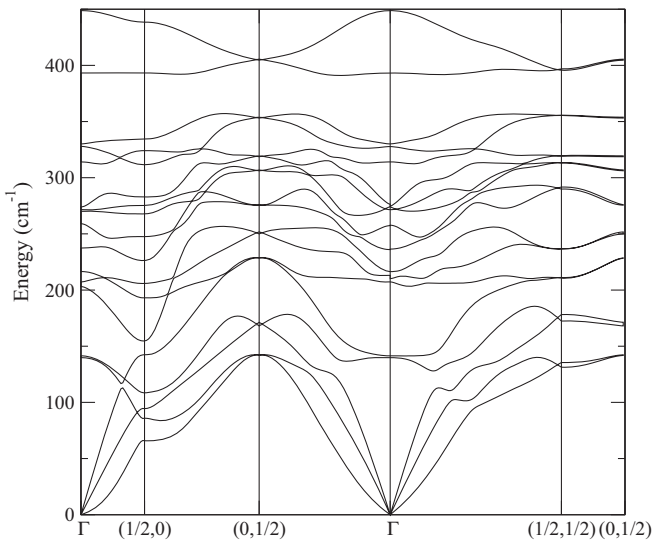


FIG. 7. Phonon dispersion of the 1T′ structure along selected directions.

## IV. CONCLUSION

Chemically and mechanically exfoliated $MoS_2$ single-layer samples have substantially different properties. While mechanically exfoliated single-layers are monophase (1H phase), the chemically exfoliated samples show the coexistence of three phases, 1H, 1T, and 1T′. The fact that three phases experimentally coexist could lead to the conclusion that the three pure structures have similar energies. However, as we have shown in the present work, this is far from being the case, as all octahedrally coordinated phases are much higher (more than 0.54 eV/Mo) in energy than the trigonal prismatic one (1H). Moreover, the pure (i.e., without adsorbates or vacancies) 1T phase is dynamically unstable and undergoes a phase transition, again with a considerable energy gain (0.29 eV/Mo), towards the most stable 1T′ structure composed of separated zigzag chains. This finding strongly questions the detection of the pure 1T phase in experiments[13,14,16] and points to a key role of either adsorbates or vacancies in stabilizing the 1T metallic structure.

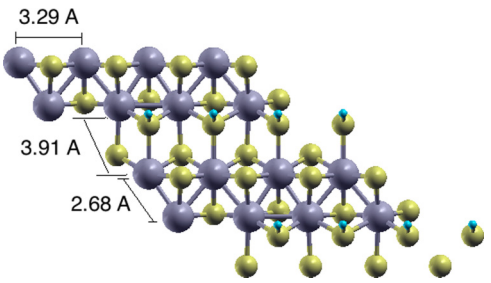


FIG. 8. (Color online) The most stable structure at 0.5 H coverage (left). The S atoms are depicted in yellow, while the hydrogen atoms are the small cyan spheres.

We have calculated dynamical properties of the lowest-energy octahedral structure (1T′) and found that it is dynamically stable, suggesting that an energy barrier does indeed exist between the 1H and 1T′ phases, similar to what happens in $WS_2$, where nudged elastic band calculations[24] find a 0.92 eV/Mo barrier between the 1T′ and 1H phases. By investigating catalytic adsorption on single-layer $MoS_2$ we demonstrate the key role of adsorbates and, more generally, of negative charging of the $MoS_2$ layer in stabilizing the 1T′ phase. This phase becomes the most stable at concentrations of $\approx$0.35 H/Mo.

Finally, we provided a microscopical description of the 1T′ Raman spectrum attributing the $J_1$, $J_2$, and $J_3$ features to specific vibrations. These features were experimentally detected in 1986,[4] but their interpretation and understanding was unknown.

Our work represents a complete study of static and lattice dynamical properties of chemically exfoliated samples. We believe that our results will be of great interest for future studies of chemically exfoliated two-dimensional crystals.

## ACKNOWLEDGMENTS

The author acknowledges useful discussions with Mannish Chhowalla and Goki Eda. The author acknowledges support from the Graphene Flagship and from the French state funds managed by the ANR within the Investissements d'Avenir program under references ANR-11-IDEX-0004-02, ANR-11-BS04-0019, and ANR-13-IS10- 0003-01. Computer facilities were provided by CINES, CCRT, and IDRIS (Project No. x2014091202).

*matteo.calandra@upmc.fr

[1] J. A. Wilson, F. J. Di Salvo, and S. Mahajan, Adv. Phys. **24**, 117 (1975).
[2] J. T. Ye, Y. J. Zhang, R. Akashi, M. S. Bahramy, R. Arita, and Y. Iwasa, Science **30**, 1193 (2012).
[3] R. F. Frindt, J. Appl. Phys. **37**, 1928 (1966).
[4] P. Joensen, R. F. Frindt, and S. R. Morrison, Mater. Res. Bull. **21**, 457 (1986).
[5] R. F. Frindt, Phys. Rev. Lett. **28**, 299 (1972).
[6] D. Yang, S. Jiménez Sandoval, W. M. R. Divigalpitiya, J. C. Irwin, and R. F. Frindt, Phys. Rev. B **43**, 12053 (1991).
[7] K. S. Novoselov, D. Jiang, F. Schedin, T. J. Booth, V. V. Khotkevich, S. V. Morozov, and A. K. Geim, Proc. Natl. Acad. Sci. USA **102**, 10451 (2005).
[8] J. N. Coleman, M. Lotya, A. O'Neill *et al.*, Science **331**, 568 (2011).
[9] M. Chhowalla, H. S. Shin, G. Eda, L. J. Li, K. P. Loh, and H. Zhang, Nat. Chem. **5**, 263 (2013).
[10] B. Radisavljevic, A. Radenovic, J. Brivio, V. Giacometti, and A. Kis, Nat. Nanotechnol. **6**, 147 (2011).
[11] M. S. Fuhrer and J. Hone, Nat. Nanotechnol. **8**, 146 (2013); A. Kis and B. Radisavljevic, *ibid.* **8**, 147 (2013).
[12] Nat. Nanotechnol. **7**, 683 (2012).
[13] G. Eda, T. Fujita, H. Yamaguchi, D. Voiry, M. Chen, and M. Chhowalla, ACS Nano **6**, 7311 (2012).
[14] G. Eda, H. Yamaguchi, D. Voiry, T. Fujita, M. Chen, and M. Chhowalla, Nano Lett. **11**, 5111 (2011).
[15] H.-P. Komsa, J. Kotakoski, S. Kurasch, O. Lehtinen, U. Kaiser, and A. V. Krasheninnikov, Phys. Rev. Lett. **109**, 035503 (2012).
[16] Y.-C. Lin, D. O. Dumcenco, Y.-S. Huang, and K. Suenaga, arXiv:1310.2363.
[17] C. Lee, H. Yan, L. E. Brus, T. F. Heinz, J. Hone, and S. Ryu, ACS Nano **4**, 2695 (2010).
[18] S. Jiménez Sandoval, D. Yang, R. F. Frindt, and J. C. Irwin, Phys. Rev. B **44**, 3955 (1991).
[19] J. P. Perdew, K. Burke, and M. Ernzerhof, Phys. Rev. Lett. **77**, 3865 (1996).
[20] P. Giannozzi *et al.*, J. Phys. Condens. Matter **21**, 395502 (2009).
[21] N. W. Ashcroft and N. D. Mermin, *Solid State Physics* (Harcourt Brace College, Fort Worth, TX, 1976).
[22] M. Boukhicha, M. Calandra, M.-A. Measson, O. Lancry, and A. Shukla, Phys. Rev. B **87**, 195316 (2013).
[23] C. Ataca and S. Ciraci, Phys. Rev. B **85**, 195410 (2012).
[24] D. Voiry, H. Yamaguchi, J. Li, R. Silva, D. C. B. Alves, T. Fujita, M. Chen, T. Asefa, V. B. Shenoy, G. Eda, and M. Chhowalla, Nat. Mater. **12**, 850 (2013).